JOURNAL OF MATERIALS SCIENCE **35** (2000) 197–201

Effect of PFT substitution on dielectric properties of PFW-PFN perovskite ceramics

B.-H. LEE, K.-K. MIN, N.-K. KIM
Department of Inorganic Materials Engineering, Kyungpook National University, Taegu 702-701, Korea
E-mail: nkkim@kyungpook.ac.kr

Perovskite phase formation and dielectric characteristics of $Pb(Fe_{2/3}W_{1/3})O_3$-$Pb(Fe_{1/2}Nb_{1/2})O_3$ ceramic system with addition of $Pb(Fe_{1/2}Ta_{1/2})O_3$ were investigated in order to examine the influence of $Pb(Fe_{1/2}Ta_{1/2})O_3$. The ceramic system powders were synthesized via a B-site precursor route. Peculiar behaviors of frequency dispersion in dielectric constant spectra in the paraelectric region were observed due to increasing conductivity. Lattice parameters, dielectric maximum temperatures, and maximum dielectric constants increased with increasing $Pb(Fe_{1/2}Nb_{1/2})O_3$ content. © *2000 Kluwer Academic Publishers*

1. Introduction

Lead-based mixed B-site cation perovskite family of $Pb(B',B'')O_3$-type (e.g., $Pb(Fe_{2/3}W_{1/3})O_3$ (PFW), $Pb(Fe_{1/2}Ta_{1/2})O_3$ (PFT), $Pb(Fe_{1/2}Nb_{1/2})O_3$ (PFN), $Pb(Mg_{1/3}Nb_{2/3})O_3$ (PMN), $Pb(Zn_{1/3}Nb_{2/3})O_3$ (PZN), etc.) are often called relaxors by intrinsic characteristics of frequency-dependent dielectric relaxation. The complex perovskite compounds and ferroelectric solid solutions thereof usually exhibit second-order-type diffuse phase transition (DPT) behavior of broad dielectric constant spectra, in contrast to the first-order sharp phase transitions of $BaTiO_3$ and $PbTiO_3$. The DPT behavior is considered to be due to local chemical inhomogeneity arising from compositional fluctuation, which indicates that structural disorder influences the phase transition modes [1–3].

Lead iron tungstate (PFW) and lead iron niobate (PFN) are reported to possess very high maximum dielectric constants of 20,000 [4, 5] and 24,000 [4, 5] at −95 °C [6–9] and 112 °C [4, 5, 10], respectively. A solid solution system of PFW-PFN has been studied widely as a potential chip capacitor material [11, 12] and the pseudobinary system became further extended with the addition of PZN [13, 14], $PbTiO_3$ [15, 16], or PMN [17]). Meanwhile, lead iron tantalate (PFT), a tantalum-analog of PFN, is also a relaxor ferroelectric with a maximum dielectric constant of 9500 [18] at −30 °C [18–20]. In the present study, PFT-modified PFW-PFN ceramic system was investigated in order to examine the effects of PFT introduction on perovskite phase formation and low-frequency dielectric characteristics.

2. Experimental

The amount of PFT added to the PFW-PFN system was fixed at 20 mol %. Compositions investigated in the present study were selected from a pseudobinary system of $(0.8 - x)$PFW-0.2PFT-xPFN (i.e., $Pb[(Fe_{2/3}W_{1/3})_{0.8-x}(Fe_{1/2}Ta_{1/2})_{0.2}(Fe_{1/2}Nb_{1/2})_x]O_3$ or $Pb[Fe_{(3.8-x)/6}Ta_{0.1}Nb_{x/2}W_{(0.8-x)/3}]O_3$), with x ranging from 0.0 to 0.8 at regular intervals of 0.2. Raw materials used were oxides of high purity; PbO (99.5%), Fe_2O_3 (99.99%), Ta_2O_5 (99.9%), Nb_2O_5 (99.9%), and WO_3 (>99%). The stoichiometry of the B-site precursor and perovskite compositions were kept as closely to the nominal values as possible by moisture compensation of raw materials as well as calcined B-site oxide powders. A B-site precursor method (synthesis of the $(B',B'')O_2$-type precursor, followed by a reaction of the product with PbO to form the perovskite structure [21, 22]), a more comprehensive and generic terminology for the so-called columbite process [23], was used in order to suppress the formation of unwanted pyrochlore phases (reported to be detrimental to dielectric properties [24]) and thereby to improve perovskite phase yields.

Overall procedures of the experiment are schematically shown in Fig. 1. Appropriate amounts of the raw materials were weighed according to the B-site precursor compositions of $[Fe_{(3.8-x)/6}Ta_{0.1}Nb_{x/2}W_{(0.8-x)/3}]O_2$, mixed, dried, calcined, and were examined using x-ray diffraction (XRD) to identify the phases formed. Thus prepared B-site precursors were then mixed with PbO also in stoichiometric proportions (without any addition of excess amount), dried, and were calcined to form perovskite phase. The steps from batch mixing to calcination were repeated once to assist the development of perovskite structures. The calcined powders were also examined using XRD and perovskite contents were estimated by comparing intensity maxima of major peaks, i.e., (110) for perovskite and (222) for pyrochlore phases. Lattice parameters of the perovskite compositions were determined from the x-ray data (with manual discrimination of the pyrochlore peaks), assuming a (pseudo)cubic structure.

The perovskite powders were mixed with binder and were pressed isostatically into pellets of ∼1 mm thick and ∼10 mm in diameter. The pellets were sintered in a double-crucible setup [25] to maintain PbO atmosphere during firing. After polishing to make parallel sides, bulk densities of the sintered specimen were determined geometrically. Dielectric constants and losses were measured on cooling (@ 4 °C/min) at 1 kHz ∼ 1 MHz under a weak oscillation level of 1.0 V, using a computer-interfaced impedance analyzer.

3. Results and Discussion

X-ray diffraction profiles of the B-site precursor powders are shown in Fig. 2. The spectrum of $x = 0.0$ (i.e., $[(Fe_{2/3}W_{1/3})_{0.8}(Fe_{1/2}Ta_{1/2})_{0.2}]O_2$) showed coexisting structures of Fe_2WO_6 (JCPDS #20-539) and $FeTaO_4$ (rutile structure, JCPDS #23-305), whilst that of $x = 0.8$ (i.e., $[(Fe_{1/2}Ta_{1/2})_{0.2}(Fe_{1/2}Nb_{1/2})_{0.8}]O_2$) was only a pattern of $FeNbO_4$ (wolframite structure, JCPDS #16-374). The $FeTaO_4$ present at that composition must have been dissolved into the wolframite structure, as the ionic radii of Ta^{5+} and Nb^{5+} are the same as 0.064 nm [26]. Since the end members of the precursor system possessed different crystal structures of Fe_2WO_6-$FeTaO_4$ and $FeNbO_4$, complete solid solutions could not be expected to form. They actually developed only limited solubility of the latter wolframite structure at $0.2 \leq x \leq 0.8$.

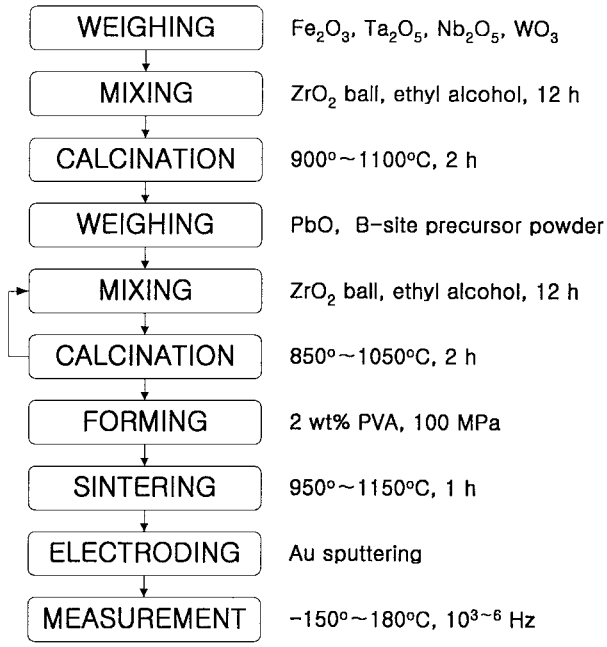

Figure 1 Block diagram of the experimental procedure.

Fig. 3 shows x-ray diffractograms of the system $(0.8 - x)$PFW-0.2PFT-xPFN. In contrast to the limited solubility of the B-site precursor system, the x-ray profiles in Fig. 3 showed well-developed crystalline solutions of a perovskite structure throughout the whole composition range, with barely detectable pyrochlore phase. Perovskite phase contents were ∼99, ∼98, and ∼100% at $0.0 \leq x \leq 0.4$, $x = 0.6$, and $x = 0.8$, respectively. Effectiveness of the B-site precursor method in the formation of perovskite powders was thus proven by such high phase purities. Meanwhile, superlattice reflection peaks could not be detected at all, indicating absence of any long-range structural ordering among octahedral cation species of Fe^{3+}, Ta^{5+}, Nb^{5+}, and W^{6+}. Since ionic radii of the four cations are quite close each other (0.0645, 0.064, 0.064, and 0.060 nm [26], respectively), ordering among them must have been greatly suppressed, as expected from the criteria proposed by Setter and Cross [27].

Lattice parameters of the (pseudo)cubic perovskite structure are plotted in Fig. 4. With increasing x (i.e., increasing PFN content, or to be more specific, increasing Nb content and decreasing Fe and W contents), the parameter of 0.3983 nm at $x = 0.0$ increased gradually to 0.4010 nm at $x = 0.8$. The steady increase at a rate of

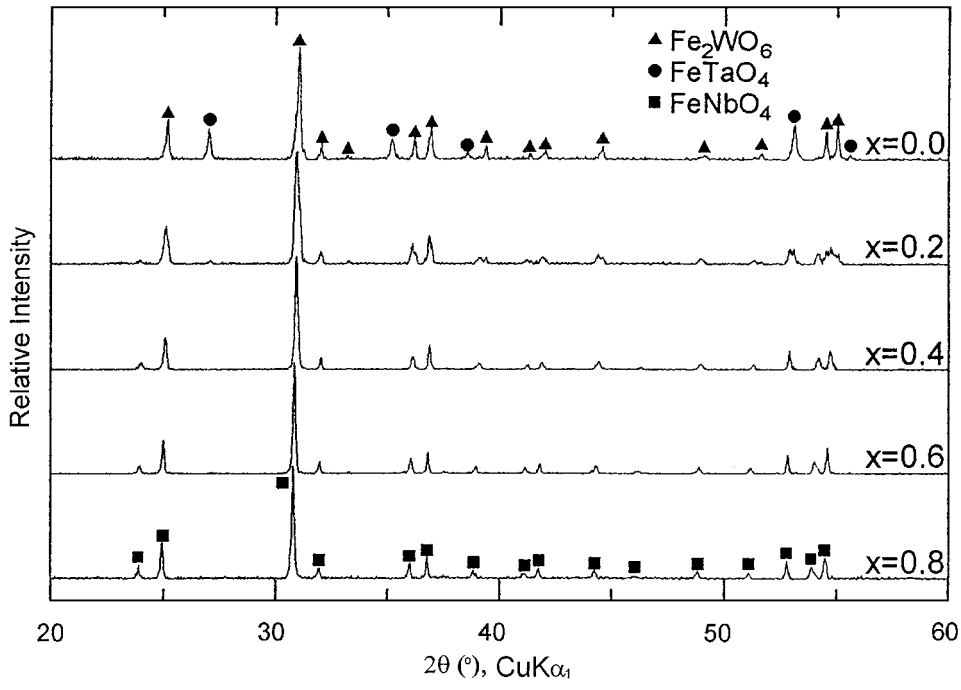

Figure 2 X-ray diffractograms of the B-site precursor system $[(Fe_{2/3}W_{1/3})_{0.8-x}(Fe_{1/2}Ta_{1/2})_{0.2}(Fe_{1/2}Nb_{1/2})_x]O_2$.

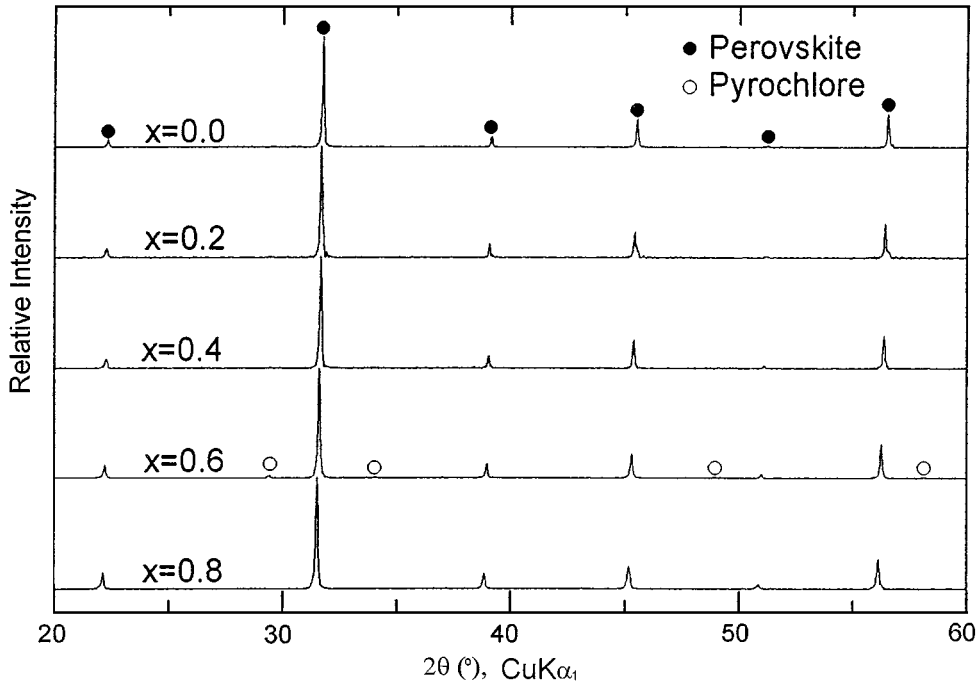

Figure 3 X-ray spectra of the $(0.8 - x)$PFW-0.2PFT-xPFN perovskite system.

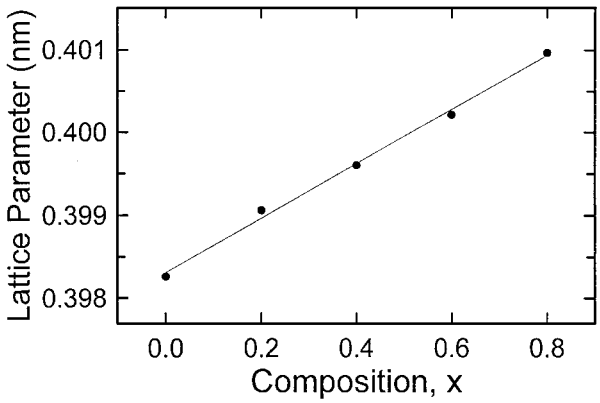

Figure 4 Variation of lattice parameters with composition change.

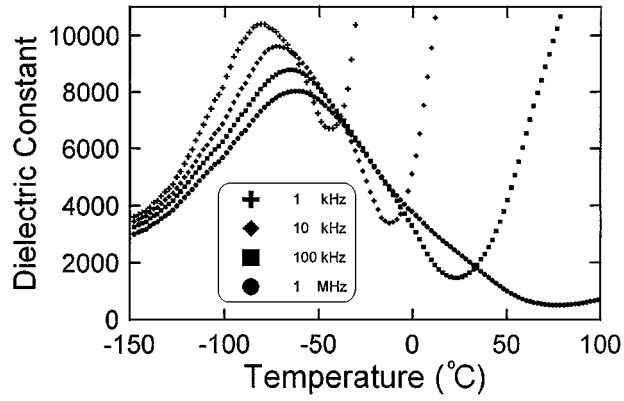

Figure 5 Dielectric constant spectra of $x = 0.0$.

0.0034 nm/mol of PFN, satisfying the Vegard's law and confirming the formation of complete solid solutions, can easily be understood by considering the octahedral ionic radii of Nb^{5+} vs. Fe^{3+} and W^{6+} (0.064 vs. 0.0645 and 0.060 nm [26]). The increasing rate in the present system is close to the rate of 0.0031 nm/mol of PFN in the PFW-PFN system [21]. The similarity can be explained by comparing the perovskite compositions of the present system and $Pb[Fe_{(4-x)/6}Nb_{x/2}W_{(1-x)/3}]O_3$ ($(1-x)$PFW-xPFN system), where the presence of PFT (20 mol %) in the present system does not influence the fractional changes of Fe, Nb, and W ions with composition change (i.e., $-x/6$, $x/2$, and $-x/3$, respectively). In other words, as the fractions of Fe, Nb, and W ions in the two systems change at the same rate (regardless of the presence of PFT), the perovskite lattices would expand accordingly. From the lattice parameters and bulk densities determined, relative densities were calculated to be 92–96%.

Representative dielectric constant spectra of composition $x = 0.0$ (i.e., $Pb[(Fe_{2/3}W_{1/3})_{0.8}(Fe_{1/2}Ta_{1/2})_{0.2}]O_3$) are displayed in Fig. 5, where frequency-dependent maximum dielectric constants (peak values of dielectric constant spectra) and dielectric maximum temperatures (temperatures corresponding to the maximum dielectric constants) at the phase transition range are clearly demonstrated. Below dielectric maximum temperatures, the dielectric constant spectra showed typical frequency dispersion behaviors of relaxor ferroelectrics. After reaching maxima, however, the dielectric constants first decreased and then increased again, which were often observed in lead-based iron-containing complex perovskite compositions [21, 28–31] and were reportedly attributed to a conduction mechanism which results in space-charge polarization [28, 31–33]. The dielectric constant spectra in the paraelectric region (prior to the recurrent increases) did not follow the same route either, unlike ordinary relaxors. Instead, the dielectric constant deviated from the rest one by one (with that of lower frequency deviating first), reached a minimum value at the changeover temperature, and then re-increased tremendously.

Moreover, minimum dielectric constant values at the changeover points decreased at very fast rates, i.e.,

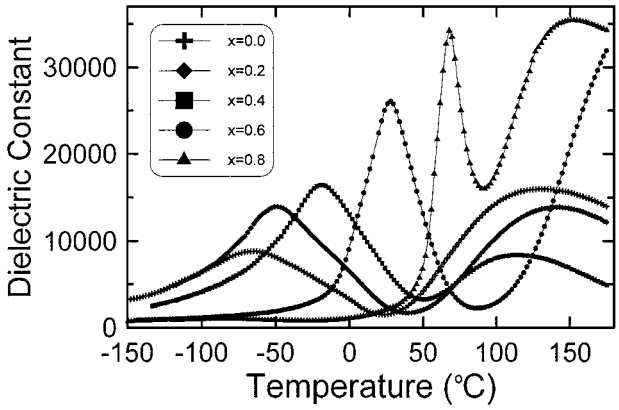

Figure 6 Dielectric constant—temperature characteristics of the perovskite system $(0.8 - x)$PFW-0.2PFT-xPFN (@100 kHz).

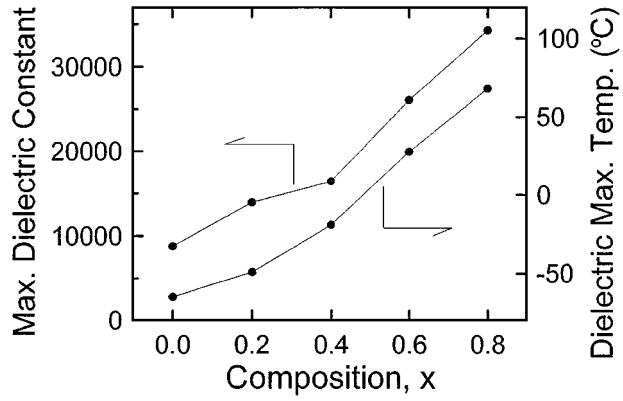

Figure 7 Dependence of maximum dielectric constant and dielectric maximum temperature upon composition (@100 kHz).

6700, 3400, 1500, and 500 at 1 kHz, 10 kHz, 100 kHz, and 1 MHz, respectively, where each value is only 1/2–1/3 (i.e., 51, 44, and 33%) of that at frequency of one decade lower. The result is in good contrast to the comparatively slower decreases in the maximum values of 10,400, 9600, 8800 and 8000 (which can be normalized as 100, 92, 85, and 77%) at dielectric maximum temperatures. Furthermore, the changeover temperatures increased more rapidly than the increases in dielectric maximum temperatures. As a result, the temperature range of normal paraelectric behavior increased steadily, i.e., 34, 60, 87, and 140 °C at the same frequency decades, which can be interpreted by the space-charge polarization, that usually occurs at frequencies of lower kHz-range [34]. Other compositions in the present system showed similar behavior of frequency dispersion.

In Fig. 6 are contrasted the dielectric constant spectra (@100 kHz) of the whole compositions, $x = 0.0$–0.8. The dielectric constant upturns occurred for all compositions in the present system as well as other perovskites, including crystallized PFW [28], PFW-PFN system [21], etc. Hence, the recurrent increases in dielectric constants in the paraelectric region seem to be inherent characteristics of iron-containing perovskites, regardless of the presence of PFT (which also contains iron) in the present study. A gradual loss of the DPT character (broad phase transitions in PFW-rich compositions became sharper and narrower with increasing PFN content), also observable in the PFW-PFN system [12, 21], is noticeable. Since intermediate compositions of the present system comprise four octahedral cation species, as compared with three species in the end components, the intermediate compositions are expected to show a greater degree of diffuseness in their phase transitions, according to Smolenskii's compositional fluctuation model [3]. Such an argument may explain the much sharper phase transition of $x = 0.8$ (as compared with other compositions), but cannot properly explain the pronounced DPT behavior at $x = 0.0$.

The maximum dielectric constant of the specimen with $x = 0.0$ was 8800 at -65 °C, whereas that for $x = 0.8$ was 34,300 at 68 °C (@ 100 kHz). Both the maximum dielectric constants and dielectric maximum temperatures increased continuously with increasing x, as separately plotted in Fig. 7. Ceramics of composition $x = 0.6$ possessed a rather high dielectric constant of 26,100 at 28 °C, quite close to room temperature. The composition might have been utilizable as a potential capacitor dielectric, were it not for the high losses of 19% (maximum value within the ferroelectric temperature range) at 20 °C and enormous increases related to the dielectric constant upturns in the paraelectric range, similar to PFW [28]. The maximum dielectric constants in the PFW-PFN system were as high as 22,800 (@ 100 kHz) for PFN-rich compositions [35], but the introduction of PFT (by 20 mol %) increased the maximum values even higher to 34,300 (∼50% as high) within the same composition range. Hence, PFT seems to play an important role in increasing the maximum dielectric constants.

4. Summary

Whereas the B-site precursor compositions developed only limited solid solubility, the perovskite system formed continuous crystalline solutions, with phase purities over 98%. Lattice parameters of the perovskite structure changed linearly with composition, which was explained in terms of fractional changes in the ionic radii of the B-site cations. All of the compositions showed relaxor behavior up to the phase transition temperatures, after which peculiar behaviors of dielectric constant spectra were observed in the paraelectric region, which was interpreted in terms of space-charge polarization. The diffuse nature in the phase transitions of the system became sharper and narrower, while dielectric maximum temperatures and maximum dielectric constants increased, with increasing PFN content. 20 mol % PFT was found to increase the maximum dielectric constant of PFN by up to ∼50%.

Acknowledgement

This work was supported by the Korea Science and Engineering Foundation (KOSEF) through the Center for Interface Science and Engineering of Materials (CISEM) at Korea Advanced Institute of Science and Technology (KAIST).

References

1. V. A. BOKOV and I. E. MYL'NIKOVA, *Sov. Phys.-Solid State* **3** (1961) 613.
2. B. N. ROLOV, *ibid.* **6** (1965) 1676.
3. G. A. SMOLENSKII, *J. Phys. Soc. Jpn.* **28** (1970) 26.
4. Y. SAKABE, in Proceedings of the MRS International Meeting on Advanced Materials, Vol. 10, Multilayers, Tokyo, Jpn., May 1988, edited by M. Doyama, S. Somiya and R. P. H. Chang (MRS, 1989) p. 119.
5. Y. YAMASHITA, *Amer. Ceram. Soc. Bull.* **73** (1994) 74.
6. V. A. BOKOV, I. E. MYL'NIKOVA and G. A. SMOLENSKII, *Sov. Phys. JETP* **15** (1962) 447.
7. G. A. SMOLENSKII and V. A. BOKOV, *J. Appl. Phys.* **35** (1964) 915.
8. YU. E. ROGINSKAYA, YU. N. VENEVTSEV and G. S. ZHDANOV, *Sov. Phys. JETP* **21** (1965) 817.
9. S. M. SKINNER, *IEEE Trans. Parts, Materials and Packaging* **PMP-6** (1970) 68.
10. I. G. ISMAILZADE, *Bull. Acad. Sci. USSR, Phys. Ser.* **22** (1958) 1480.
11. M. YONEZAWA, K. UTSUMI and T. OHNO, in Proceedings of the First Meeting on Ferroelectric Materials and their Applications, Kyoto, Jpn., 1977, p. 297.
12. H. TAKAMIZAWA, K. UTSUMI, M. YONEZAWA and T. OHNO, *IEEE Trans. CHMT* **CHMT-4** (1981) 345.
13. M. YONEZAWA, K. UTSUMI and T. OHNO, in Proceedings of the Second Meeting on Ferroelectric Materials and their Applications, Kyoto, Jpn., 1979, p. 215.
14. M. YONEZAWA, *Amer. Ceram. Soc. Bull.* **62** (1983) 1375.
15. S.-L. FU and G.-F. CHEN, *ibid.* **66** (1987) 1397.
16. G. F. CHEN and S.-L. FU, *J. Mater. Sci.* **23** (1988) 3258.
17. S.-G. JUN, M.S. thesis, Kyungpook National Univ., Taegu, Korea, 1996.
18. S. NOMURA, H. TAKABAYASHI and T. NAKAGAWA, *Jpn., J. Appl. Phys.* **7** (1968) 600.
19. G. A. SMOLENSKII, A. I. AGRANOVSKAYA and V. A. ISUPOV, *Sov. Phys.-Solid State* **1** (1959) 907.
20. A. I. AGRANOVSKAYA, *Bull. Acad. Sci. USSR, Phys. Ser.* **24** (1960) 1271.
21. B.-H. LEE, N.-K. KIM, J.-J. KIM and S.-H. CHO. *Ferroelectrics* **211** (1998) 233.
22. B.-H. LEE, N.-K. KIM, B.-O. PARK and S.-H. CHO, *Mater. Lett.* **33** (1997) 57.
23. S. L. SWARTZ and T. R. SHROUT, *Mater. Res. Bull.* **17** (1982) 1245.
24. T. R. SHROUT and A. HALLIYAL, *Amer. Ceram. Soc. Bull.* **66** (1987) 704.
25. M.-C. CHAE, N.-K. KIM, J.-J. KIM and S.-H. CHO, *Ferroelectrics* **211** (1998) 25.
26. R. D. SHANNON, *Acta Cryst.* **A32** (1976) 751.
27. N. SETTER and L. E. CROSS, *J. Mater. Sci.* **15** (1980) 2478.
28. N. K. KIM and D. A. PAYNE *J. Mater. Res.* **5** (1990) 2045.
29. W. HUEBNER, W. R. XUE and P. W. LU, in Proceedings of the 9th IEEE International Symposium on Applications of Ferroelectrics, University Park, USA, August 1994, edited by R. K. Pandey, M. Liu and A. Safari (IEEE, 1994) p. 150.
30. S.-G. JUN, N.-K. KIM, J.-J. KIM and S.-H. CHO, *J. Kor. Phys. Soc.* **32** (1998) S1002.
31. N. ICHINOSE and N. KATO, *Jpn. J. Appl. Phys.* **33** (1994) 5423.
32. T. R. SHROUT, S. L. SWARTZ and M. J. HAUN, *Amer. Ceram. Soc. Bull.* **63** (1984) 808.
33. K. SAKATA and H. TAKAHARA, *Jpn. J. Appl. Phys.* **26**(2) (1987) 83.
34. W. D. KINGERY, H. K. BOWEN and D. R. UHLMANN, "Introduction to Ceramics," 2nd ed. (John Wiley & Sons, New York, 1976) p. 923.
35. M.-C. CHAE and N.-K. KIM, *Ferroelectrics* **209** (1998) 603.

Received 17 October 1997
and accepted 16 July 1999